BILINGUAL PUBLISHING GROUP

Journal of Environmental & Earth Sciences

https://journals.bilpubgroup.com/index.php/jees

ARTICLE

The Mekkam Inlier (Eastern Morocco): A Magmatic Domain with Mixed Characteristics: Contribution of Petrographic and Geochemical Data

Gouiss Abdelali [1*] **, *Souad M'rabet*** [1] **, *Ali Lhachmi*** [2]**, *Youness Taybi*** [3] **, *Youssef Gharmane*** [4,5]

[1] *Geosciences Laboratory, Faculty of Sciences, Ibn Tofaïl University, P.O. Box 133, Kenitra 14000, Morocco*

[2] *Polydisciplinary Faculty of Taza, Natural Resources and Environment Laboratory, Department of Geology, Sidi Mohamed Ben Abdellah University, Fez 1223, Morocco*

[3] *LCM2E Lab Géo-Environnement et Santé, Multidisciplinary Faculty of Nador, Mohamed First University, P.O. Box 300, Selouane 62702, Morocco*

[4] *Higher School of Technology, Sultan Moulay Slimane University of Beni Mellal, P.O. Box 336, Fkih Ben Salah 23000, Morocco*

[5] *Multidisciplinary Research and Innovation Laboratory, Faculté Polydisciplinaire Khouribga, Sultan Moulay Slimane University of Beni Mellal, P.O. Box 145, Khouribga 25000, Morocco*

ABSTRACT

The Mekkam inlier is located 50 km southeast of the town of Taourirt, in northeastern Morocco. It offers a great opportunity for the study of Variscan magmatism in Morocco. This inlier is punctuated by small magmatic bodies which we will characterize through a petrographic and geochemical study to situate this inlier in its geotectonic context. The petrographic study revealed the existence of three trends: acidic, intermediate, and basic, which are represented by facies ranging from granites to basanites, including andesites, rhyolites, trachytes, dacites, quartz microdiorites, Aplite and microgranites. All these facies have a mineralogical assemblage dominated by quartz, plagioclase, oligoclase, potassium feldspar, pyroxene, and biotite; the most abundant accessory minerals are zircon and apatite. Green hornblende is found in

*CORRESPONDING AUTHOR:

Gouiss Abdelali, Geosciences Laboratory, Faculty of Sciences, Ibn Tofaïl University, P.O. Box 133, Kenitra 14000, Morocco;
Email: abdelali.gouiss@uit.ac.ma

ARTICLE INFO

Received: 17 November 2024 | Revised: 22 November 2024 | Accepted: 28 November 2024 | Published Online: 22 January 2025
DOI: https://doi.org/10.30564/jees.v7i2.7784

CITATION

Abdelali, G., M'rabet, S., M'rabet, A., et al., 2025. The Mekkam Inlier (Eastern Morocco): A Magmatic Domain with Mixed Characteristics: Contribution of Petrographic and Geochemical Data. Journal of Environmental & Earth Sciences. 7(2): 49–61. DOI: https://doi.org/10.30564/jees.v7i2.7784

microdiorites and dacites. The geochemical analysis, conducted through the examination of major elements, trace elements, and rare earth elements, has uncovered the presence of two distinct magmatic series: a calc-alkaline series of the island arc type or active continental margin, and another alkaline series of syn-collision. Based on this combined data, we propose that the Mekkam sector represents a magmatic arc developed within a compressional tectonic regime located above a subduction zone, which was later followed by an intracontinental collision phase.

Keywords: Mekkam; Petrography; Geochemistry; Eastern Meseta; Morocco

1. Introduction

The Paleozoic Inlier of Mekkam, the object of this study (**Figure 1**), is part of the Eastern Moroccan Meseta linked to the Variscan chain. The inlier appears as an erosion window through a Meso-Cenozoic cover located 50 km SE of the city of Taourirt (northeastern Morocco). In the Eastern Meseta, magmatic activity is expressed by intrusions of granitoids deposited at different levels in the Paleozoic series. The ages of emplacement of these plutons are close: 348.1 ± 2.3 at Zekarra[1], 344 ± 60 at Tanncherfi[2], 321 ± 19 at Merguechoum[3], 328 ± 19 at Tarilest[4], 308.2 ± 2.7 at Beni Snassene[1], and 287 ± 7 at Soulouina[5]. Their links with the phases of Variscan structuring are the same. They also have significant mineralogical and geochemical differences. Several petrographic, structural, and geochemical studies have been carried out on these plutons in the Eastern Meseta[5–10], whereas the Mekkam inlier has been little studied due to the restriction of its outcrops. The magmatic manifestations of the Mekkam include: (1) small plutons, dykes and sills at Sidi Lahcen crossing the Devonian schists to the north, (2) the Hassiane Ed Diab-Soulouina series with metric-sized granitoid pointements to the south, and (3) the Zerroug volcano-sedimentary complex, which also outcrops south of the inlier. In previous geological studies of the region[11–18], only a few petrographic and geochemical studies have been conducted. The region has never been the object of a detailed petrographic study, and its geotectonic context has never been discussed. It is in this context that the inlier was targeted with the following objectives:

1. establish petrographic characteristics to identify rock types and their mineralogical composition.
2. specify rock geochemistry (major elements, trace elements and rare earth elements).
3. determine geotectonic implications.

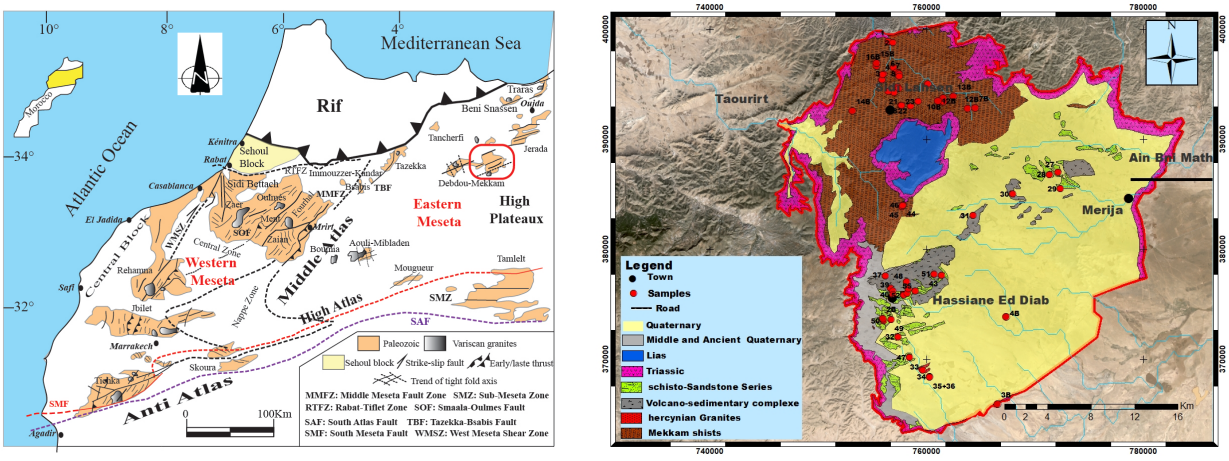

Figure 1. Location of the study area. (**a**) Position of the study area on the structural map of the different Hercynian domains in northern Morocco[19]. (**b**) Simplified geological map of the Mekkam inlier.

2. Geological Setting

The geological setting of the study area is part of the Moroccan Eastern Meseta. The latter represents what remains of the Variscan chain in Morocco, following the collision of the two main continents Laurussia to the north and Gondwana to the south, during the Upper Paleozoic under a transpressive tectonic regime[20, 21]. The Variscan orogeny was formed over a variable time interval between the Terminal Devonian and the Upper Carboniferous. During this period, the Rheic Ocean to the north and the Medio-European Ocean to the south were subducted to form the gigantic continent of Pangea[20, 21]. This is reflected regionally in the Eastern Meseta by early deformation followed by significant magmatism in the Lower Carboniferous[22]. Lower Visean granodiorites and rhyodacites are the most dominant facies in this region[23]. Locally in the Mekkam region, outcrops vary in nature and age. The schists of Mekkam which occupy the entire northern part of the inlier (Sidi Lahcen area) are a thousand-metre-thick series consisting of olive-green or violet schists alternating with beds of sandstone and greywacke[11]. Palynological studies by Marhoumi et al.[14] have given this series a Middle Devonian age. The volcano-sedimentary series from Zerroug to Hassiane Ed Diab occupies almost the southern half of the inlier and consists of extensive eruptive material underlain by detrital and carbonate levels of Upper Visean age[18]. The work of Remmal[17] has shown that this series can be divided into three sets: a basal unit corresponding to the first layers of the Carboniferous series, the volcanoclastites of Jbel Zerroug superimposed on the detrital and carbonate base levels, and the Hassiane Ed Diab-Soulouina series, which extends beyond a major E-W fault that limits the Jbel Zerroug complex to the south. According to our observations, these ancient terrains are unconformably covered by Triassic formations and Quaternary deposits.

The structural context of the Mekkam region is marked by polyphase deformation[24], characterized by the combined effects of Variscan and Atlasic deformation, resulting in the emergence of a variety of ductile and brittle tectonic structures such as faults, folds, and associated schistosity. The sequence of these tectonic events led to two episodes of Variscan deformation, D1 and D2[16], the most significant of which was dated at 368 Ma using the K/Ar method[25]. In addition to these two episodes, there is a third episode D3 of deformation of Westphalian C age[16]. The episode D1 corresponds to the major structuring of the Mekkam shale. The episode D2 is the second episode of deformation in the sector, probably occurring during the Breton phase and predating the Upper Visean deposits[11]. The D3 episode is late Hercynian, dated to the Westphalian C[15].

3. Material and Method

Field missions were the first step in this work, where all magmatic occurrences were surveyed with a total of 76 rock samples representing the various rock types found in the Mekkam region. A mineralogical and petrographic study has enabled their identification. Then, 14 unaltered samples were selected to cover the entire region for geochemical analysis (major, trace, and rare earth elements) by X-ray fluorescence spectroscopy (XRF) for major elements and inductively coupled plasma mass spectrometry (ICP-MS) for trace elements and rare earth elements at the Reminex research center in Guelmassa (Managem, Marrakech, Morocco). Chemical analyses of major elements in percent oxide weight, as well as trace elements and rare earths in ppm, are shown in **Table 1**.

4. Results

4.1. Petrography

Macroscopic and microscopic observations of all facies in the three major regions of Sidi Lahcen, Jbel Zerroug and Hassiane Ed Diab show the presence of a notable petrographic variety.Primary mineralogy is represented by quartz, plagioclase, potassium feldspar, pyroxene and biotite. Amphibole is found in microdiorites and dacites. The most abundant accessory minerals are zircon and apatite. Hydrothermal alteration has been observed in most of the samples, linked to the low-grade epizonal metamorphism affecting the province. This alteration contributes to the appearance of a secondary paragenesis represented by chlorite and calcite, The original texture of magmatic facies is generally well preserved. The specific petrographic features of the three regions are shown below.

(1) To the north, in the Sidi Lahcen region, the outcrops appear as dykes and sills oriented E-W for the microgranites, rhyolites, and dacites and NW-SE for the microdiorite

Table 1. Geochemical analyses of magmatic rocks from the Mekkam inlier.

Samples	HD 5B	HD 6B	SL 23	SL 25	SL 26	SL 7B	HD 48	HD 41	SL 3	SL 5	SL 14	HD 9	SL 24	HD 36
%														
SiO_2	41.16	41.2	47.67	54.38	54.7	65.09	68.02	74.07	75.52	74.41	75.39	74.69	72.85	73.36
TiO_2	3.48	3.48	1.48	1.56	0.71	0.49	0.3	0.16	0.045	0.36	0.046	0.12	0.19	0.023
Al_2O_3	13.41	13.43	13.48	16.66	15.68	16.05	16.53	14.14	14.09	14.89	14.3	14.07	14.22	14.78
Fe_2O_3	15.3	15.3	8.59	7.34	5.98	3.92	3.1	4.48	0.81	2.87	2.33	0.72	1.88	0.67
MnO	0.22	0.22	0.19	0.2	0.19	0.13	0.096	0.012	0.045	0.013	0.032	0.021	0.085	0.011
MgO	8.28	8.27	7.19	3.16	5.82	1.79	1.11	0.32	0.11	0.32	0.17	0.32	0.59	0.057
CaO	10.15	10.17	10.58	5.19	4.6	1.47	1.47	0.2	0.42	0.15	0.17	0.51	0.6	0.62
Na_2O	3.51	3.52	3.09	3.55	3.75	3.07	6	0.16	3.14	0.26	2.24	3	3.17	3.42
K_2O	1.25	1.25	2.1	2.84	1.14	3.96	1.9	3.78	4.73	4.19	3.09	5.4	4.96	6.37
P_2O_5	0.93	0.92	1.31	0.35	0.22	0.17	0.098	0.065	0.047	0.17	0.043	0.088	0.12	0.088
SO_3	0.25	0.24	3.05	0.18	0.03	0.15	0.021	0.083	0.029	0.053	0.22	0.011	0.012	0.03
Loi	1.83	1.78	0.87	4.45	7.03	3.39	1.33	2.41	1.01	2.14	1.96	0.98	1.19	0.6
Total	99.77	99.78	99.6	99.86	99.85	99.68	99.975	99.88	99.996	99.826	99.991	99.93	99.867	100.02
ppm														
As	40.62	11.81	12.56	16.88	196.62	12.17	148.26	97.56	49.28	25.23	156.41	22.86	32.39	186.63
B	15.09	14.46	28.82	26.44	21.1	15.48	12.46	19.25	0.92	9.84	3.01	1.35	6.61	3.37
Ba	736.2	735.43	586.92	545.09	365.72	3240.4	462.27	983.62	153.9	1131.9	269.5	628.44	699.64	128.74
Be	1.45	1.35	2.04	2.08	1.29	2.87	1.02	3.23	8.11	0.65	4.15	2.93	3.8	3.93
Bi	<0.1	<0.1	<0.1	<0.1	<0.1	<0.1	<0.1	5.81	1.07	14.35	5.46	<0.1	<0.1	<0.1
Cd	<0.1	<0.1	<0.1	<0.1	<0.1	<0.1	<0.1	<0.1	<0.1	<0.1	<0.1	<0.1	<0.1	<0.1
Ce	91.59	93.03	177.66	67.31	56.69	72.11	40.98	55.26	11.26	63.02	13.78	42.52	53.48	24.57
Co	43.06	43.31	24.58	17.32	12.48	8.78	7.31	4	12.04	11.16	5.32	2.63	4.01	2.72
Cr	135.88	134.61	140.11	62.83	228.3	62.63	72.75	105.2	21.34	51.74	40.68	66.01	74.9	112.37
Cs	0.24	0.25	22.99	6.72	2.34	4.21	4.5	8.02	5.25	6.32	7.59	7.34	5.3	4.97
Cu	43.36	44.65	38.26	27.1	21.57	42.53	23.73	196.49	20.52	30.07	60.99	28.56	13.37	13.85
Dy	5.62	5.69	3.22	4.78	2.51	2.94	1.08	2.77	1.46	2.49	1.1	2.01	2.48	3.29
Er	2.19	2.25	1.27	2.49	1.24	1.48	0.48	1.36	0.82	1.26	0.64	1.04	1.29	1.57
Eu	3.26	3.32	2.65	1.77	1.4	4.07	0.87	0.98	0.2	0.82	0.45	0.79	1.18	0.13
Ga	23.14	22.36	20.29	21.13	19.95	20.23	20.86	22.15	18.49	22.04	19.23	15.9	18.1	20.55
Gd	8.68	8.74	7.22	5.63	3.5	4.5	1.85	4.01	1.37	3.62	1.14	2.58	2.87	3.43
Ge	<0.1	<0.1	<0.1	<0.1	<0.1	<0.1	<0.1	<0.1	<0.1	<0.1	<0.1	<0.1	<0.1	<0.1
Hf	1.38	1.4	1.24	1.85	1.46	18.9	1.9	4.27	0.94	2.16	1.5	1.7	4.17	1.12
Ho	0.79	0.8	0.45	0.78	0.41	0.48	0.19	0.43	0.27	0.4	0.21	0.34	0.42	0.5
La	42.74	43.56	74.47	30.84	25.29	39.13	21.02	23.26	5.19	33.49	6.95	18.21	18.45	9.46
Li	17.4	17.69	76.62	68.07	91.14	36.18	44.52	21.13	36.15	21.42	18.56	26.05	38.65	12.49
Lu	0.2	0.2	0.11	0.31	0.14	0.23	0.058	0.24	0.14	0.19	0.11	0.15	0.19	0.22
Mo	3.73	3.57	2.65	4.16	3.71	5.39	4.76	6.38	1.44	3.68	3.39	6.09	4.19	7.12
Nb	17.93	16.04	16.06	17.06	17.41	16.64	11.22	15.51	93.38	11.1	11	64.07	46.28	19.92
Nd	48.72	49.4	76.31	30.22	23.57	27.57	14.29	22.06	5.89	22.43	6	15.51	16.12	14.21
Ni	129.71	130.71	151.11	15.16	82.84	31.46	24.98	13.8	9.11	8.83	15.24	11.33	83.64	30.02
Pb	4.84	5.99	25.5	45.93	40.06	11.36	28.87	12.45	56.59	219.82	77.58	41.63	69.55	34.53
Pr	10.81	10.94	21.26	7.26	5.83	7.14	3.92	5.75	1.57	6.14	1.66	4.3	4.41	3.57
Rb	24.12	23.89	27.99	109.36	43.7	158	57.2	297.21	257.09	196.15	237.76	214.19	179.62	231.9
Sb	1.03	0.88	0.77	<0.1	0.6	<0.1	0.24	0.53	4.18	0.61	0.58	0.2	0.49	0.28
Sc	15.65	15.48	15.72	15.37	13.52	6.53	4.46	4.59	4.02	6.1	3.69	3.2	4.58	6.2
Se	<0.1	<0.1	<0.1	<0.1	<0.1	<0.1	<0.1	<0.1	<0.1	1.36	<0.1	<0.1	<0.1	<0.1
Sm	9.81	9.9	10.33	5.97	4.06	4.89	2.23	4.65	1.64	4.09	1.42	3.11	3.26	4.55
Sn	1.03	1.97	13.9	1.22	<0.1	0.93	<0.1	<0.1	<0.1	1.91	<0.1	4.14	0.34	<0.1
Sr	1049.2	1051.7	2122.1	452.4	446.58	299.38	260.44	25.88	45.39	95.2	63.74	108.37	152.76	34.26
Ta	2.37	2.38	1.09	0.95	0.83	0.49	0.41	0.26	0.34	0.21	0.18	0.21	0.44	0.49
Tb	1.03	1.04	0.68	0.76	0.42	0.51	0.2	0.51	0.22	0.43	0.17	0.34	0.39	0.53
Th	3.63	3.63	8.81	9.94	10.05	17.91	12.38	17.17	9.12	18.4	6.5	13.34	15.37	16.3
Tm	0.27	0.27	0.15	0.36	0.17	0.23	0.066	0.22	0.14	0.19	0.1	0.16	0.2	0.25
U	0.99	0.96	2.13	2.39	2.85	5.34	3.11	3.74	5.02	6.77	5.5	4.1	5.46	4.24
V	193.47	194.04	156.2	112.17	101.73	48.96	36.3	55.47	0.8	38.47	2.08	11.65	18.16	6.67
W	3.03	2.61	2.92	2.4	2.78	2.47	1.96	10.13	9.45	56.53	8.78	6	3.63	5.33
Y	20.06	20.08	11.64	20.56	10.14	13.47	4.48	11.53	6.7	11.1	5.03	9.11	11.27	12.61
Yb	1.68	1.68	0.91	2.44	1.13	1.62	0.45	1.64	1.11	1.39	0.83	1.16	1.43	1.81
Zn	129.71	131.13	99.73	112.59	112.12	53.22	53	35.95	47.18	29.63	49.05	75.72	75.7	30.46
Zr	242.68	254.05	160.07	238	127.73	98.56	96.21	82.31	85.05	271.17	50.99	58.57	75.79	59.03

dykes. The relative chronology shows that the microdiorite dykes are the oldest since in the field, the microdiorites are intersected by the other dykes. The most represented facies in this region are:

a) The quartzitic microdiorite (SL25) with a porphyritic microgranular texture. It is composed of the following mineral assemblage: plagioclase, amphibole, biotite, quartz, rare orthoclase crystals and accessory minerals. The plagioclase corresponds to the most represented mineral phase, and they are subautomorphic, of andesine type (An 30 to 40%). The mesostasis is microgranular, showing a relatively high crystallization rate containing microcrystals of quartz surrounded by a fine halo of secondary minerals such as calcite and oxides. This facies shows strong alteration, highlighted by the presence of calcite and chlorite (**Figure 2a**).

b) The micro-gabbrodiorite (SL23) exhibits a microgranular texture with dominant plagioclase (An 25 to 30%) with a little alkaline feldspar of the microcline type. The ferromagnesian mineral is green amphibole with automorphic patches, giving the rock its mesocratic color (**Figure 2b**).

c) The microgranite (SL24) has a porphyritic microgranular texture with the presence of slightly perthitic alkali feldspar phenocrysts, automorphic to subautomorphic quartz, altered plagioclase, and chloritized biotite in a micrograined

mesostasis composed mainly of feldspars and quartz (**Figure 2c**).

d) The aplite (SL14) is vacuolar leucocratic and slightly oxidized. Under the microscope the rock is primarily composed of subautomorphic quartz grains with recrystallized edges and rosette-shaped muscovite, sometimes associated with hematite (**Figure 2d**).

e) The rhyolite (SL3) has a weathering rind with a color that varies from pink to white. The rock is composed of automorphic quartz phenocrysts, alkali feldspar, and plagioclase in a microlitic quartz-feldspathic micaceous matrix (**Figure 2e**).

f) The andesites (SL26) are less represented in the Sidi Lahcen area. They are identifiable by the abundant presence of plagioclase crystals and their purple hue. They also contain crystals of amphibole and biotite, which are often altered to chlorite. Their matrix is composed of microlites and microcrystals of plagioclase.

g) The dacites (SL 7B) are composed of phenocrysts of fully sericitized plagioclase, altered green hornblende, chloritized biotite, and globular quartz. The mesostasis is microlitic (**Figure 2f**).

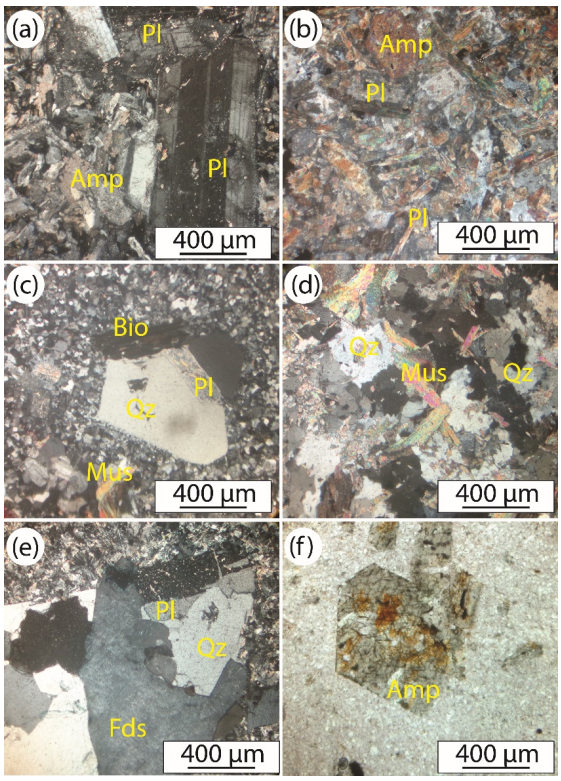

Figure 2. Petrography of the main facies of Sidi Lahcen: (**a**) microdiorite, (**b**) micro-gabbrodiorite, (**c**) microgranite, (**d**) aplite, (**e**) rhyolite, (**f**) dacite.

(2) To the south of the study area, between the village of Hassiane Ed Diab and the Soulouina region, extends a schist-sandstone series of Upper Visean age [17]. Through this series, outcrop points of an underlying granitic massif are observed. In this region, facies are represented by:

a) The biotite microgranite of Ras-Mohamed (HD9), which has a porphyritic microgranular texture characterized by zoned automorphic plagioclase phenocrysts of oligoclase type (An 30%). These plagioclase crystals cluster into several contiguous individuals, forming feldspathic aggregates sometimes reaching up to 3 cm. These plagioclase crystals are slightly altered. The quartz is automorphic to subautomorphic. At its edges, it associates with plagioclase to form myrmekite, indicating a eutectic syncrystallization between feldspar and quartz. These myrmekites make up the matrix of the microgranite. The biotite is in the form of laths with numerous inclusions of apatite and metamict zircons (**Figure 3a,b**).

b) The Soulouina granite (HD36) is pinkish leucocratic with a granular texture. It is composed of acidic plagioclases, alkali feldspars, quartz, and a few rare biotite. Myrmekite is observed along the edges of the alkali feldspars. Zircon and hematite are accessory minerals (**Figure 3c,d**).

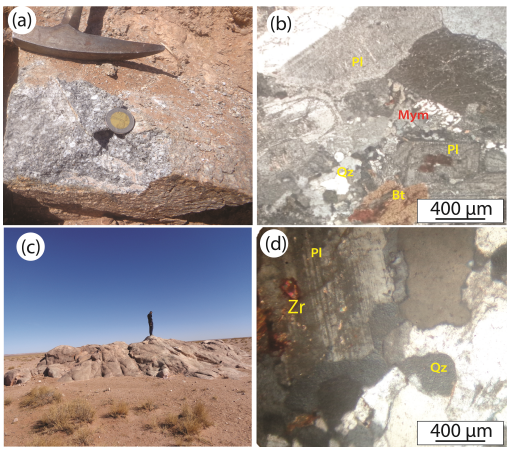

Figure 3. Petrography of the granitoids of Hassiane Ed Diab: (**a**,**b**) microgranite, (**c**,**d**) granite.

(3) The volcanic-sedimentary complex of Jbel Zerroug, has slightly undulating and elongated SW-NE reliefs, with the highest point at Jbel Zerroug (1314 m). The general appearance of outcrops is characterized by scree [26]. The main facies of this complex are:

a) The trachyte (HD48) has a porphyritic microlitic texture. The main minerals are potassium feldspar, plagio-

clase, green amphibole often altered to chlorite and calcite, and occasional patches of black mica. The matrix is feldspathic microlitic. Oxides are scattered throughout the rock (**Figure 4a**).

b) The rhyolite (HD41) outcrops to the east of the village of Hassiane Ed Diab in the form of a pull-apart structure; the rock varies in color from pink to dark pink. It exhibits a porphyritic texture where the main minerals are automorphic quartz, sericitized alkali feldspar, greenish biotite, and a few rare amphiboles. The groundmass is feldspathic. The rock is altered with the development of hematization and sericitization (**Figure 4b**).

c) The andesite exhibits a massive texture composed of the following mineralogy: oligoclase-type plagioclase (An 25–30%), in the form of microlites, green amphibole, and clinopyroxene as microphenocrysts. Their matrix is microlitic (**Figure 4c**).

d) The basanite (HD5B) has a microlitic texture composed of phenocrysts of plagioclase (An 35 to 42%), pyroxene, olivine, and nepheline, with a microlitic matrix primarily formed by plagioclase microlites. The accessory minerals are epidote and oxides (**Figure 4d**).

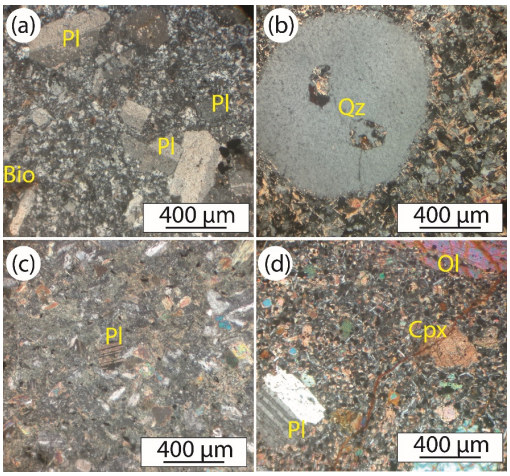

Figure 4. Petrography of the main facies at Jbel Zerroug: (**a**) trachyte, (**b**) rhyolite, (**c**) andesite, (**d**) basanite.

4.2. Geochemistry

4.2.1. Major Elements

The chemical analyses of the samples (**Table 1**) reveal a generally low percentage loss of ignition (LOI) between 0.6 and 4.45%, except for sample SL26 (andesite) with a rate of 7.03%. The rocks are therefore slightly altered and close to the line of fresh rocks. The projection of the different facies(HD4B, HD5B, SL3, SL26, HD7B, HD48, HD41) using the TAS classification diagram of Bas et al.[27] reveals that the volcanic rocks occupy the fields of ultrabasic rocks for basanite, intermediate rocks for andesite, and acidic rocks for dacite, rhyolite, and trachyte. These facies exhibit a calc-alkaline lineage and an alkaline affinity for the basanites (**Figure 5**). The range of major element composition varies among these three groups:

- Basanites have the following composition: SiO_2 around 41 wt.%, TiO_2 (3.48 wt.%), Al_2O_3 (13.41 wt.%), Fe_2O_3 (15.3 wt.%), MgO (8.3 wt.%), CaO (10.17 wt.%), Na_2O (3.52 wt.%), K_2O (1.25 wt.%), and P_2O_5 (0.9 wt.%). These geochemical characteristics are comparable to Quaternary-aged basanites recently described by Bosch et al.[28] and Bernard-Griffiths et al.[29].
- Intermediate rocks have SiO_2 contents of 54.38 wt.%. The other oxides have the following contents: Fe_2O_3 (5.98%), CaO (4.6%), MgO (5.82%), and TiO_2 (0.7%).
- The acid volcanic rocks have high contents of SiO_2 (65.09–75.72 wt.%), Al_2O_3 (14.09–16.53 wt.%), Na_2O (0.1–6 wt.%), and K_2O (1.9–4.73 wt.%), and low percentages of CaO (<1.47 wt.%), MgO (<1.79 wt.%), TiO_2 (<0.49 wt.%), and variable for Fe_2O_3 (0.43–2.35 wt.%). The rhyolites have a relatively high content of K_2O (4.73 wt.%), which is attributed to the alteration of feldspar into sericite. These geochemical characteristics are similar to volcanic rocks described in the Western Meseta by Hadimi et al.[30] and Ntarmouchant et al.[31].

The projection of the different facies (SL23, SL25, SL5, SL14, SL24, HD9, HD36) using the TAS diagram[32] for classifying plutonic rocks shows that microgranites, aplites and granites fall within the granite field, microdiorites within the diorite field, and micro-gabbrodiorites within the gabbro field. These granitoids are affiliated with a calc-alkaline lineage, while the granites of Soulouina, micro-gabbrodiorites, and microdiorites fall within an alkaline lineage (**Figure 6**). The plutonic rocks have higher contents of SiO_2 ranging from 72.85 to 74.69 wt.%, Al_2O_3 (14.07 to 14.78 wt.%), Na_2O (0.26 to 3.42 wt.%), and K_2O (4.19 to 6.37 wt.%). These rocks have lower contents of CaO (0.15–0.62 wt.%),

MgO (0.057–0.59 wt.%), Fe_2O_3 (0.67–2.87 wt.%), and TiO_2 (0.023–0.36 wt.%). Microdiorites and micro-gabbrodiorites have the following compositions: SiO_2 (47.67–54.38 wt.%), TiO_2 (1.48–1.56 wt.%), Al_2O_3 (13.48–16.66 wt.%), Fe_2O_3 (7.34–8.59 wt.%), MgO (3.16–7.19 wt.%), CaO (5.19–10.58 wt.%), Na_2O (3.09–3.5 wt.%), K_2O (2.1–2.84 wt.%), P_2O_5 (0.35–1.31 wt.%). These geochemical characteristics are similar to the granites described in the Moulay Bouazza region of the Western Meseta by Oudy et al.[33] and in the Tanncherfi inlier, located 40 km north of Mekkam[2].

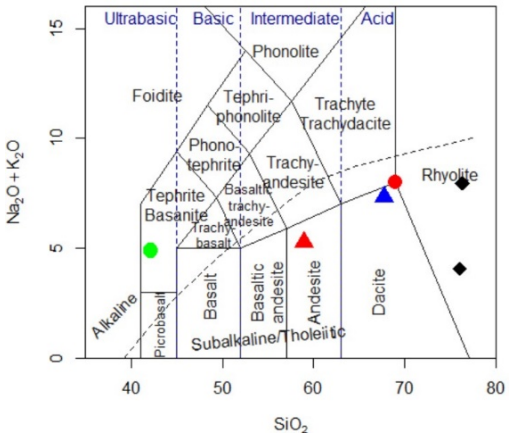

Figure 5. Classification of volcanic rocks from the study area, TAS diagram[27].

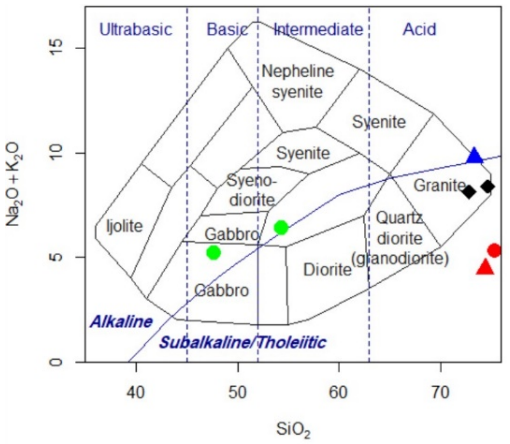

Figure 6. Classification of plutonic rocks, total alkali versus silica diagram[32].

4.2.2. Trace Elements and Rare Earth Elements (REE)

The multi-element diagrams normalized to primitive mantle[34] revealed the following observations:

The spectra of the granitoids show enrichment in Rb, Cs and a negative anomaly in Ba, Nb, and Ti, with a positive anomaly in Pb (**Figure 7a**). The anomaly in Nb on the normalized diagrams of the primitive mantle is widely used to examine the effects of either crustal contamination of the lithosphere or the subducted slab in magmatic processes. In the granitoids of Mekkam, the presence of this negative anomaly indicates an orogenic nature associated with a subduction zone[35, 36]. According to Thompson et al.[37], La/Nb values suggest the influence of crustal contamination. These values range between 0.5 and 7 in arc settings. The granitoids of Mekkam have La/Nb values of 3.01 with modest Th/Nb ratios of 1.65 and Th/La ratios of 0.54, which could suggest that they originate from a mantle source with contamination by the continental crust in a geodynamic context of an island arc or active continental margin. The spectra obtained for the microdiorites and micro-gabbrodiorites are slightly different. The negative Nb anomaly is present, characteristic of orogenic volcanism (**Figure 7a**). This orogenic nature is also confirmed by the low quantities of transition elements (V, Cr, Ni, and Sc)[38]. Thus, the high values of La/Nb ratios exceeding 1.8 (2.4–4.81), the values of Zr/Y ratios exceeding 3 (4.91–5.58), and the low values of Ti/Y ratios (2.66–3.63) characterize an orogenic magmatism in an active continental margin context[39].

The spectra obtained for the volcanic rocks (rhyolite, trachyte, and andesite) reveal marked similarities despite differences in their mineralogical compositions and degrees of differentiation. Compared to the primitive mantle, the profiles show a negative anomaly in Nb and Ti, characteristic of orogenic volcanism (**Figure 7b**). These rocks exhibit positive anomalies in Rb and negative anomalies in Nb, suggesting that their formation occurred in a convergent margin setting[34]. The enrichment in LILE (Ba, Pb, Rb) and depletion in HFSE (Nb, Ta, Lu, Eu, Y) suggest that these rocks are similar to those formed in a subduction zone or post-collision continent-continent collision setting[39] (**Figure 7b**).

The spectra of dacites show a positive anomaly in Ba, Pb, Nd, and Eu, and a negative anomaly in Ti and P. This negative anomaly can be explained by prior fractionation of iron-titanium oxides and apatite.

In the basanites, the spectra are different, with the presence of a positive Ba and Ti anomaly (**Figure 7b**) and an enrichment of elements (Sr, Nd, Zr, Ti), indicating that these rocks are intraplate in nature[40]. These characteristics are identical to the Quaternary basanites generated in an

intraplate context in the Middle Atlas [41].

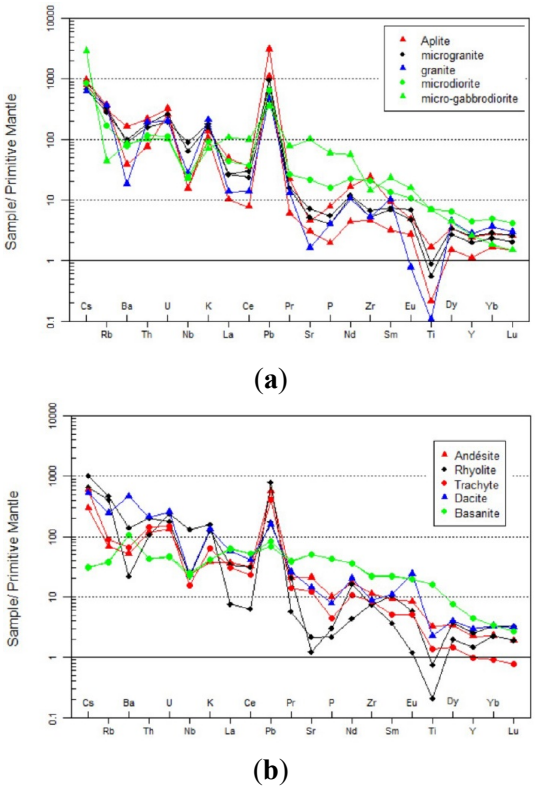

Figure 7. Multi-element diagram normalized to the primitive mantle [34]. (**a**) Plutonic rocks (**b**) Volcanic rocks.

4.2.3. Geotectonic Setting

- For volcanic rocks, the diagram from Cabanis [42] is highly effective in characterizing magmatic series and their geotectonic environment. Some trace elements and potassium are normalized to MORB.N (Mid-Ocean Ridge Basalt). The volcanic rocks are associated with the orogenic domain linked to a compressive active margin context and the post-orogenic domain linked to a compressive intraplate magmatism context (**Figure 8**). Thus, in the diagram by Pearce, Harris and Tindle [43], acidic volcanic rocks (rhyolite and dacite) project into the orogenic granitoids of volcanic arcs. This indicates the orogenic context of subduction and their formation in a tectonically active zone, confirmed by their calc-alkaline nature. The Zerroug basanites occupy the domain of active margins and show different characteristics from the other group, confirming the different context of these facies already discussed in the previous section.
- Regarding granitoids, the use of diagrams from Pearce, Harris and Tindle [43] allows for distinguishing between four groups: volcanic arc granites (VAG) and syn-collision (Syn-COLG) granites, associated with the convergent orogenic domain; ocean ridge granites (ORG), linked to divergent zones; and within-plate granites (WPG) from the anorogenic intraplate domain.

The projection of data from the Mekkam inlier onto these diagrams shows that most of the granitoids occupy the domain of volcanic arc granites (**Figure 9**), likely associated with continental margin subduction or an evolved stage of island arc development. The Soulouina granite occupies the field of syn-collision granitoids, this agrees with their geochemical signatures.

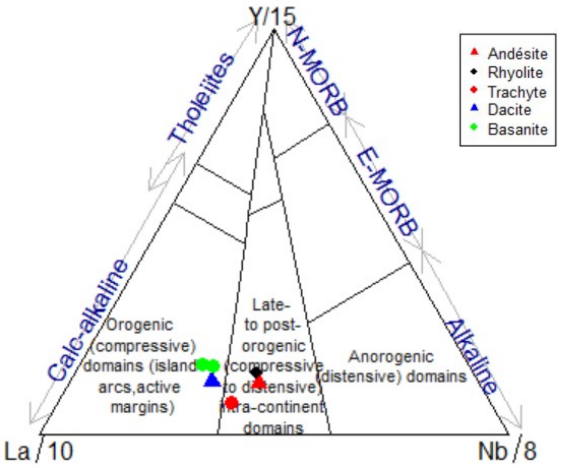

Figure 8. Mekkam facies projection in the diagram of Cabanis [42].

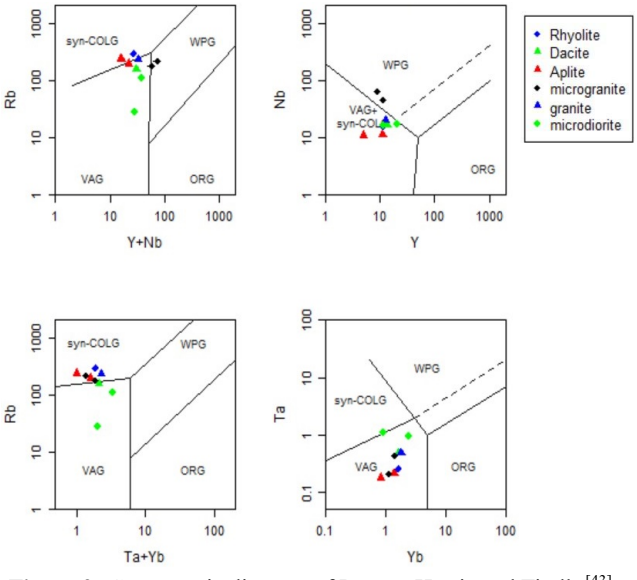

Figure 9. Geotectonic diagram of Pearce, Harris and Tindle [43].

5. Discussion

The origin of Variscan magmatism in Morocco remains a topic of discussion to this day, and several hypotheses have been proposed to explain the genesis of this magmatism. Authors such as Kharbouch et al.[44] and Boulin, Bouabdelli and El Houicha[45] propose an ocean-continent subduction. Other authors[18, 26, 46] adopt the hypothesis of an intracontinental subduction. Subsequently, some authors[38, 47–49] interpreted the Moroccan Meseta domain as foreland or back-arc basins. The recent work of Michard et al.[50] proposes a southeast-directed subduction of the Rheic Ocean crust along the Iberian and Moroccan Meseta. Accotto et al.[51] suggest the hypothesis of an Avalonian magmatic arc in relation to a northwest-directed subduction.

The recent model by Chopin et al.[1] explains the chronology of the Variscan granitoids of the Moroccan Meseta as linked to the early Carboniferous extensional event resulting from the fragmentation of Gondwana associated with the opening of the Paleotethys. Then, during the remainder of the Carboniferous and the early Permian, a Variscan intracontinental collision occurred in two stages, indicating the onset of the collision between Gondwana and the European Variscan belt.

This study, based on petrological and geochemical arguments, reveals that the Mekkam inlier is part of the Variscan magmatism of the eastern and western Moroccan Meseta, with the presence of an initial alkaline magmatic event preceding a calc-alkaline orogenic magmatism linked to a volcanic arc context (microdiorite alkaline Sidi Lahcen and calc-alkaline rhyolites & andesite Sidi Lahcen and Hassiane Ed Diab). This is followed by a post- to late-orogenic alkaline magmatism associated with an active continental margin (Soulouina Granite). This is consistent with studies conducted at the scale of the Eastern Meseta[1] and Western Meseta[33]. These events unfolded as follows:

1. The first magmatic event is orogenic and likely occurred during the Late Visean, associated with a significant volcanic episode during which the Zerroug volcanic series and the microdiorite dykes of Sidi Lahcen were deposited. This magmatic event is comparable to magmatic events widespread in the Eastern Meseta[1, 2, 52] and Western Meseta[53–55].

2. The second event is syn-orogenic, marked by the emplacement of alkaline granite and late-stage dykes at Sidi Lahcen. The presence of this event is also reported in the Eastern Meseta[1, 5, 18] and Western Meseta[30, 56, 57].

3. After these Paleozoic episodes, the area experienced a long period of stability. Then, magmatic activity resumed in the form of alkaline-affinity basic volcanism (basanites of Hassiane Ed Diab), as described in other areas throughout the Mediterranean[28, 58].

In this geodynamic framework, the first event can be interpreted as associated with a magmatic arc in a compressional setting above the subduction zone. This is consistent with the model of Michard et al.[50]. The second event is related to the Variscan intracontinental collision in the Meseta, which occurred in two stages at the end of the Carboniferous and the beginning of the Permian[59]. The third event is related to the Quaternary magmatism in Morocco affecting the Mediterranean periphery, generated in an intraplate geotectonic context[41, 58, 60].

6. Conclusions

The Mekkam inlier has remained understudied to date due to its remoteness and due to its covering by Mesozoic and Cenozoic overburden, which reveals some exposures of the Paleozoic crystalline basement. Field observations and petrographic data combined with geochemistry have shown that magmatic activity in the Mekkam inlier exhibits two phases: volcanism associated with calc-alkaline plutonism of island arc or active continental margin subduction type, followed by subsequent intraplate alkaline volcanism.

Comparing the obtained results with studies conducted in similar regions in the Eastern and Western Meseta allows to highlighting the succession of magmatic events in this region.

Utilizing all the data suggests that the Mekkam sector corresponds to a magmatic arc in a compressional domain situated above the subduction zone, followed by intracontinental collision. These results are consistent wit the hypotheses proposed for the tectonic framework of the Moroccan Meseta.

Author Contributions

Conceptualization, methodology, software, and writing, G.A.; conceptualization, methodology, software, and writing, S.M.; visualization, investigation, and reviewing,

A.L.; reviewing and software, Y.T.; reviewing, Y.G.

Funding

This research received no external funding.

Institutional Review Board Statement

Not applicable.

Informed Consent Statement

Not applicable.

Data Availability Statement

The authors agree to share their research data.

Conflicts of Interest

The authors declare no conflict of interest.

References

[1] Chopin, F., Leprêtre, R., El Houicha, M., et al., 2023. U–Pb geochronology of Variscan granitoids from the Moroccan Meseta (Northwest Africa): Tectonic implications. Gondwana Research. 117, 274–294. DOI: https://doi.org/10.1016/j.gr.2023.02.004

[2] Ajaji, T., Weis, D., Giret, A., et al., 1998. Coeval potassic and sodic calc-alkaline series in the post-collisional Hercynian Tanncherfi intrusive complex, northeastern Morocco: geochemical, isotopic and geochronological evidence. Lithos. 45(1–4), 371–393. DOI: https://doi.org/10.1016/S0024-4937(98)00040-1

[3] Rafi, A., 1988. Approche pétrographique, géochimique et géochronologique (Rb/Sr) des granitoïdes du Maroc oriental [Ph.D. Thesis]. Marrakech, MA: Cadi Ayyad University. p. 139. (in French)

[4] Mrini, Z., Rafi, A., Duthou, J.-L., et al., 1992. Chronologie Rb-Sr des granitoides hercyniens du Maroc; consequences. Bulletin of the Geological Society of France. 163(3), 281–291.

[5] Tisserant, D., 1977. Les isotopes du strontium et l'histoire hercynienne du Maroc, Étude de quelques massifs atlasiques et mésétiens. Strasbourg, France: Université Louis Pasteur-Strasbourg I. 60p. (in French).

[6] Elabouyi, M., Dahire, M., Driouch, Y., et al., 2019. Crustal anatexis in the Aouli-Mibladen granitic complex: A window into the middle crust below the Moroccan Eastern Variscan Meseta. Journal of African Earth Sciences. 154, 136–163. DOI: https://doi.org/10.1016/j.jafrearsci.2019.03.006

[7] El Hadi, H., Reddad, A., Giret, A., et al., 2000. Place des massifs granitiques de Zekkara, Tarilest et Béni-Snassène dans l'histoire géodynamique de la chaîne hercynienne (Meseta orientale, Maroc). Géologie Méditerranéenne. 27(3), 159–173. (in French).

[8] El Hadi, H., Tahiri, A., Reddad, A., 2003. Les granitödes hercyniens post-collisionnels du Maroc oriental: Une province magmatique calco-alcaline à shoshonitique. Comptes Rendus Geoscience. 335(13), 959–967. (in French). DOI: https://doi.org/10.1016/j.crte.2003.09.003

[9] EL Hadi, H., Simancas, J.F., Tahiri, A., et al., 2006. Comparative review of the Variscan granitoids of Morocco and Iberia: proposal of a broad zonation. Geodinamica Acta. 19(2), 103–116.

[10] Gharmane, Y., Hinaje, S., Amrani, S., et al., 2023. Tectonic fracturing and paleostress reconstruction in the Tazekka Variscan massif (Morocco): Implications for magmatic processes. Proceedings. Physical and Natural Sciences. 34(4), 1169–1184. DOI: https://doi.org/10.1007/s12210-023-01190-0

[11] Desteucq, C., Hoepffner, C., 1980. Déformations hercyniennes dans les boutonnières paléozoïques de Debdou et du Mekam (Maroc Oriental). Mines, Géologie et Énergie. 48, 93–99. (in French).

[12] Medioni, R., 1980. Mise au point stratigraphique sur les terrains carbonifères de la bordure septentrionale des Hauts-Plateaux marocains (Massif de Debdou, boutonnières de Lalla-Mimouna et du Mekam). Notes and Memoirs of the Geological Survey of Morocco c. 41(285), 25–37. (in French).

[13] Huvelin, P., 1983. Plutonisme acide à Sidi Lahcen (Paléozoïque du Mekam, région d'Oujda, Maroc oriental) et présence de cornéennes recoupées par des filons à scheelite et wolframite ou à molybdénite. Proceedings of the Academy of Sciences, Series 2, Mechanics, Physics, Chemistry, Sciences of the Universe, Earth Sciences. 297(1), 57–62. (in French).

[14] Marhoumi, M.R., Hœpffner, C., Doubinger, J., et al., 1983. Données nouvelles sur l'histoire hercynienne de la Meseta orientale au Maroc: l'âge dévonien des schistes de Debdou et du Mekam. Proceedings of the Academy of Sciences, Series 2, Mechanics, Physics, Chemistry, Sciences of the Universe, Earth Sciences. 297(1), 69–72. (in French).

[15] Chegham, A., 1985. Etude minéralogique et géologique des filons Pb-Zn-Ag (Fe, Cu, Bz) de Sidi Lahcen (Boutonnière de Mekam, Maroc Oriental) [Ph.D. Thesis]. Orléans, France: Université d'Orleans. p. 280. (in French).

[16] Hoepffner, C., 1987. La tectonique hercynienne dans l'Est du Maroc [Ph.D. Thesis]. Strasbourg. pp. 1–257.

(in French).

[17] Remmal, T., 1989. Etude métallogènique des indices wolframifères du district de Hassiane Diab, région d'Oujda (Maroc nord oriental) [Ph.D. Thesis]. Nancy, France: Institut National Polytechnique de Lorraine. 256p. (in French).

[18] Kharbouch, F., 1994. Les laves dévono-dinantiennes de la méseta marocaine: Etude pétro-géochimique et implications géodynamiques. Brest, France: Université de Bretagne occidentale, 191p. (in French).

[19] Hoepffner, C., Soulaimani, A., Piqué, A., 2005. The moroccan hercynides. Journal of African Earth Sciences. 43(1–3), 144–165. DOI: https://doi.org/10.1016/j.jafrearsci.2005.09.002

[20] Arthaud, F., Matte, P., 1977. Late Paleozoic strike-slip faulting in southern Europe and northern Africa: Result of a right-lateral shear zone between the Appalachians and the Urals. Geological Society of America Bulletin. 88(9), 1305–1320.

[21] Pa, Z., 1989. Evolution of Laurussia. A study in the late palaeozoic plate tectonics. Kluver Academic Publishers: Dordrecht, Netherlands. pp. 1–102.

[22] Bouabdellah, M., 2011. Touissit-Bou Beker, un district Pb-Zn de type Mississippi Valley dans la Chaîne des Horsts (Maroc oriental). Nouveaux Guides Géologiques et Miniers du Maroc. 9, 325–330. (in French).

[23] Hoepffner, C., Houari, M.R., Bouabdelli, M., 2006. Tectonics of the North African Variscides (Morocco, western Algeria): An outline. Comptes Rendus Geoscience. 338(1–2), 25–40. DOI: https://doi.org/10.1016/j.crte.2005.11.003

[24] Gouiss, A., Taybi, Y., Gharmane, Y., et al., 2023. Contribution of Space Remote Sensing and new GIS tools for mapping geological structures in the Mekkam region of Northeast Morocco. Geographia Technica. 18(2), 149–157. DOI: https://doi.org/10.21163/gt_2023.182.11

[25] Huon, S., 1985. Clivage ardoisier et réhomogénéisation isotopique K-Ar dans les schistes paléozoïques du Maroc. Etude microstructurale et isotopique, conséquences régionales [Ph.D. Thesis]. Strasbourg, France: Université de Strasbourg. pp. 125. (in French).

[26] Chalot-Prat, F., 1990. Petrogenese d'un volcanisme intracontinental tardi-orogenique hercynien: Etude d'un complexe volcanique carbonifere du tazekka et de zones volcaniques comparables dans le mekam et la region de jerada (maroc oriental) [Ph.D. Thesis]. Paris, France: Université Pierre et Marie Curie. 283p. (in French).

[27] Bas, M.J.L.E., Le Maitre, R.W., Streckeisen, A., et al., 1986. A chemical classification of volcanic rocks based on the total alkali-silica diagram. Journal of Petroleum. 27(3), 745–750.

[28] Bosch, D., Maury, R.C., Bollinger, C., et al., 2014. Lithospheric origin for neogene–quaternary middle Atlas lavas (Morocco): Clues from trace elements and Sr–Nd–Pb–Hf isotopes. Lithos. 205, 247–265. DOI: https://doi.org/10.1016/j.lithos.2014.07.009

[29] Bernard-Griffiths, J., El Azzouzi, M., Bellon, H., et al., 1999. Evolution des sources du volcanisme marocain au cours du Néogène. Comptes Rendus of the Academy of Sciences, Series II A: Earth and Planetary Sciences. 329(2), 95–102. (in French).

[30] Hadimi, I., Youbi, M., Lahna, A.A., et al., 2021. U–Pb zircon geochronological and petrologic constraints on the post-collisional variscan volcanism of the Tiddas-Souk Es-Sebt des Aït Ikko basin (Western Meseta, Morocco). Minerals. 11(10), 1099. DOI: https://doi.org/10.3390/min11101099

[31] Ntarmouchant, A., Smaili, H., Bento dos Santos, T., et al., 2016. New evidence of effusive and explosive volcanism in the Lower Carboniferous formations of the Moroccan Central Hercynian Massif: Geochemical data and geodynamic significance. Journal of African Earth Sciences. 115, 218–233. DOI: https://doi.org/10.1016/j.jafrearsci.2015.12.019

[32] Cox, K.G., Bell, J.D., Pankhurst, R.J., 1979. The interpretation of igneous rocks. Chapman & Hall, London, p. 450.

[33] Oudy, A., Ouazzani, H., Ouabid, M., et al., 2023. Petrography and geochemistry of the Moulay Bouazza granitoids (Moroccan Variscan central massif). Implications for their origin and geodynamic setting. Journal of African Earth Sciences. 104939. DOI: https://doi.org/10.1016/j.jafrearsci.2023.104939

[34] Sun, S.-S., McDonough, W.F., 1989. Chemical and isotopic systematics of oceanic basalts: Implications for mantle composition and processes. Geological Society of London, Special Publications. 42(1), 313–345. DOI: https://doi.org/10.1144/GSL.SP.1989.042.01.19

[35] Saunders, A.D., Storey, M., Kent, R.W., et al., 1992. Consequences of plume-lithosphere interactions. Geological Society of London, Special Publications. 68(1), 41–60. DOI: https://doi.org/10.1144/GSL.SP.1992.068.01.04

[36] Gower, C.F., Swinden, H.S., 1991. Pillow lavas in the Dead Islands area, Grenville province, southeast Labrador. Current Research, Newfoundland Department of Mines and Energy, Geological Survey Branch, Report. 91(1), 205–215.

[37] Thompson, R.N., Morrison, M.A., Hendry, G.L., et al., 1984. An assessment of the relative roles of crust and mantle in magma genesis: An elemental approach. Philosophical Transactions of the Royal Society of London, Series A: Mathematical, Physical and Engineering Sciences. 310(1514), 549–590.

[38] Bennouna, A., 2006. Evolution tectono-sédimentaire et magmatique du dépocentre volcano-sédimentaire carbonifère du massif du Tazekka (Moyen-Atlas, Maroc):

Implications pour l'évolution géodynamique des hercynides marocaines [Ph.D. Thesis]. Fès, Morocco: Université Sidi Mohammed Ben Abdellah. 208p. (in French).

[39] Condie, K.C., 1989. Geochemical changes in basalts and andesites across the Archean-Proterozoic boundary: Identification and significance. Lithos. 23(1–2), 1–18.

[40] Pearce, J.A., 1982. Trace element characteristics of lavas from destructive plate boundaries. In: Thorpe, R.S. (ed.). Orogenic Andesites and Related Rocks. John Wiley and Sons: Hoboken, NJ, USA. pp. 528–548.

[41] Benamrane, M., Santos, J.F., Mata, J., et al., 2023. The alkaline intraplate Pliocene-Quaternary lavas from the Middle Atlas Volcanic Field (Morocco): Petrology, mineralogy and geochemistry. Journal of African Earth Sciences. 205, 105014. DOI: https://doi.org/10.1016/j.jafrearsci.2023.105014

[42] Cabanis, B., 1989. Le diagramme La/10–Y/15–Nb/8: un outil pour la discrimination des séries volcaniques et la mise en évidence des processus de mélange et/ou de contamination crustale. Comptes Rendus L'Académie des Sciences. Série 2, 2023. (in French).

[43] Pearce, J.A., Harris, N.B.W., Tindle, A.G., 1984. Trace element discrimination diagrams for the tectonic interpretation of granitic rocks. Journal of Petrology. 25(4), 956–983. DOI: https://doi.org/10.1093/petrology/25.4.956

[44] Kharbouch, F., Juteau, T., Treuil, M., et al., 1985. Le volcanisme dinantien de la Meseta marocaine nord-occidentale et orientale. Caractères pétrographiques et géochimiques et implications géodynamiques. Geological Sciences, Bulletin Memoirs. 38(2), 155–163. (in French).

[45] Boulin, J., Bouabdelli, M., El Houicha, M., 1988. Evolution paléogéographique et géodynamique de la chaîne paléozoïque du Moyen-Maroc: un essai de modélisation. Comptes Rendus de l'Académie des Sciences. Série 2, Mécanique, Physique, Chimie, Sciences de l'Univers, Sciences de la Terre. 306(20), 1501–1506. (in French).

[46] Lagarde, J.-L., 1987. Les plutons granitiques hercyniens marqueurs de la déformation crustale: L'exemple de la méseta marocaine [Ph.D. Thesis]. Rennes, France: Université de Rennes 1. 379p. (in French).

[47] Ben Abbou, M., Soula, J.-C., Brusset, S., et al., 2001. Contrôle tectonique de la sédimentation dans le système de bassins d'avant-pays de la Meseta marocaine. Comptes Rendus of the Academy of Sciences, Series II A: Earth and Planetary Sciences. 332(11), 703–709. (in French).

[48] Roddaz, M., Brusset, S., Soula, J.C., et al., 2002. Foreland basin magmatism in the Western Moroccan Meseta and geodynamic inferences. Tectonics. 21(5), 1–7. DOI: https://doi.org/10.1029/2001TC901029

[49] Essaifi, A., Samson, S., Goodenough, K., 2014. Geochemical and Sr–Nd isotopic constraints on the petrogenesis and geodynamic significance of the Jebilet magmatism (Variscan Belt, Morocco). Geological Magazine. 151(4), 666–691. DOI: https://doi.org/10.1017/S0016756813000654

[50] Michard, A., Soulaimani, A., Hoepffner, C., et al., 2010. The south-western branch of the Variscan Belt: Evidence from Morocco. Tectonophysics. 492(1–4), 1–24. DOI: https://doi.org/10.1016/j.tecto.2010.05.021

[51] Accotto, C., Poyatos, D.M., Azor, A., et al., 2020. Tectonic evolution of the Eastern Moroccan Meseta: From Late Devonian forearc sedimentation to Early Carboniferous collision of an Avalonian promontory. Tectonics. 39(7), e2019TC005976. DOI: https://doi.org/10.1029/2019TC005976

[52] Oukemeni, D., 1993. Géochimie, géochronologie (U-Pb) du pluton d'Aouli et comparaisons géochimiques avec d'autres granitoïdes hercyniens du Maroc par analyse discriminante [Ph.D. Thesis]. Sherbrooke, Canada: Université du Québec à Chicoutimi. 141p. (in French).

[53] Delchini, S., Lahfid, A., Lacroix, B., et al., 2018. The geological evolution of the Variscan Jebilet Massif, Morocco, inferred from new structural and geochronological analyses. Tectonics. 37(12), 4470–4493. DOI: https://doi.org/10.1029/2018TC005002

[54] Ait Lahna, A., Aarab, E., Youbi, N., et al., 2018. The Lalla Tittaf Formation (Rehamna, Morocco): Paleoproterozoic or Paleozoic age. Proceedings of the ICG2018-Joint Congress-CAAWG9-CAAWG9-ArabGU2-ICGAME3; 20 to 24–March, 2018; Faculty of Sciences El Jadida, (El Jadida, Morocco). pp. 13–16.

[55] Essaifi, A., Potrel, A., Capdevila, R., et al., 2003. Datation U/Pb: Âge de mise en place du magmatisme bimodal des Jebilet centrales (chaîne Varisque, Maroc). Implications géodynamiques. Comptes Rendus Géoscience. 335(2), 193–203. (in French). DOI: https://doi.org/10.1016/S1631-0713(03)00030-0

[56] Domeier, M., Font, E., Youbi, N., et al., 2021. On the Early Permian shape of Pangea from paleomagnetism at its core. Gondwana Research. 90, 171–198.

[57] Hadimi, I., Youbi, N., Ait Lahna, A., et al., 2018. U-Pb zircon geochronological and petrologic constraints on the Post-collisional variscan volcanism of the Khenifra basin (Western Meseta, Morocco). Proceedings of the 2nd International Congress on Permian and Triassic Stratigraphic and Petrogenetic Implications; 25 to 27–April, 2018; Faculty of Sciences Ben M'sik, (Casablanca, Morocco). pp. 53–54.

[58] El Azzouzi, M., Bernard-Griffiths, J., Bellon, H., et al., 1999. Evolution of the sources of Moroccan volcanism during the Neogene. Proceedings of the Academy of Sciences, Series 2, Mechanics, Physics, Chemistry, Sciences of the Universe, Earth Sciences. 95–102.

[59] Chopin, F., Corsini, M., Schulmann, K., et al.,

2014. Tectonic evolution of the Rehamna metamorphic dome (Morocco) in the context of the Alleghanian-Variscan orogeny. Tectonics. 33(6), 1154–1177. DOI: https://doi.org/10.1002/2014TC003539

[60] Benamrane, M., Németh, K., Jadid, M., et al., 2022. Geomorphological classification of monogenetic volcanoes and its implication to tectonic stress orientation in the Middle Atlas Volcanic Field (Morocco). Land. 11(11), 1893. DOI: https://doi.org/10.3390/land11111893